Report

Current Biology

Intrinsic Cell Polarity Coupled to Growth Axis Formation in Tobacco BY-2 Cells

Graphical Abstract

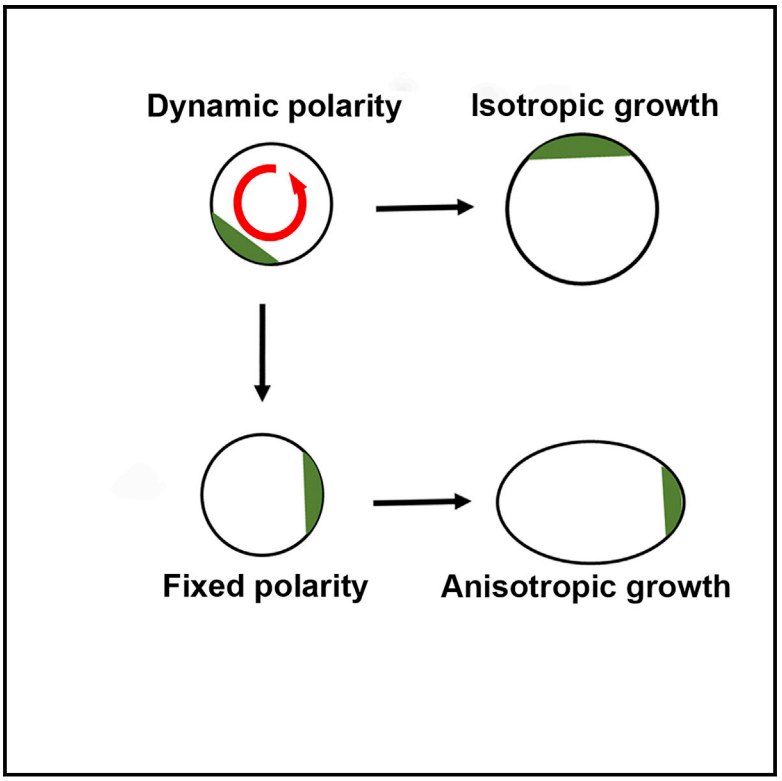

Highlights

- Ectopic GFP-BASL reveals a polarized molecular address in tobacco suspension cells
- Spherical protoplasts have an intrinsic ability to polarize
- Polarity is aligned with growth in regenerating protoplasts growing anisotropically
- Polarity is dynamic in regenerating protoplasts growing isotropically

Authors

Jordi Chan, Catherine Mansfield, Flavie Clouet, Delfi Dorussen, Enrico Coen

Correspondence

jordi.chan@jic.ac.uk (J.C.), enrico.coen@jic.ac.uk (E.C.)

In Brief

Chan et al. reveal a polarized molecular address in tobacco suspension cells through ectopic expression of GFP-BASL. They show protoplasts have an intrinsic ability to polarize and that polarity is aligned with the growth axis as they regenerate. Tissue-wide cues may bias the direction of polarity and thus orient anisotropic growth.

Chan et al., 2020, Current Biology *30*, 4999–5006
December 21, 2020
https://doi.org/10.1016/j.cub.2020.09.036

CellPress

Current Biology

CellPress
OPEN ACCESS

Report

Intrinsic Cell Polarity Coupled to Growth Axis Formation in Tobacco BY-2 Cells

Jordi Chan,[1,*] Catherine Mansfield,[1] Flavie Clouet,[1] Delfi Dorussen,[1] and Enrico Coen[1,2,*]
[1]John Innes Centre, Colney Lane, Norwich NR4 7UH, UK
[2]Lead Contact
*Correspondence: jordi.chan@jic.ac.uk (J.C.), enrico.coen@jic.ac.uk (E.C.)
https://doi.org/10.1016/j.cub.2020.09.036

SUMMARY

Several plant proteins are preferentially localized to one end of a cell, allowing a polarity to be assigned to the cell. These cell polarity proteins often exhibit coordinated patterns between neighboring cells, termed tissue cell polarity. Tissue cell polarity is widespread in plants and can influence how cells grow, divide, and differentiate [1–5]. However, it is unclear whether cell polarity is established through cell-intrinsic or -extrinsic mechanisms and how polarity is coupled to growth. To address these issues, we analyzed the behavior of a tissue cell polarity protein BASL (BREAKING OF ASYMMETRY IN THE STOMATAL LINEAGE) in the simplifying context of cultured cell filaments and in protoplasts before and during regeneration. We show that BASL is polarly localized when ectopically expressed in tobacco BY-2 cell cultures. Ectopic BASL is found preferentially at the developing tips of cell filaments, likely marking a polarized molecular address. Polarity can shift during the cell cycle and is resistant to treatment with microtubule, actin or auxin transport inhibitors. BASL also exhibits polar localization in spherical protoplasts, in contrast to other polarity proteins so far tested. BASL polarity within protoplasts is dynamic and resistant to auxin transport inhibitors. As protoplasts regenerate, polarity remains dynamic in isotropically growing cells but becomes fixed in anisotropic cells and aligns with the axis of cell growth. Our findings suggest that plant cells have an intrinsic ability to polarize and that environmental or developmental cues may act by biasing the direction of this polarity and thus the orientation of anisotropic growth.

RESULTS AND DISCUSSION

Several plant proteins exhibit preferential localization at one end of a cell, allowing the cell to be assigned a polarity. The location of these polarity proteins is often coordinated between neighboring cells such that, for a given protein, polarities point in similar or opposing directions in a region of tissue. Coordinated tissue cell polarity plays a key role in diverse developmental processes, including phyllotaxy, venation, stomatal patterning, and growth [1–5]. These findings raise the question of how tissue cell polarity is established and coordinated. One hypothesis is that cells have an intrinsic ability to polarize, and signaling between cells then acts to coordinate polarities between neighbors [6]. Alternatively, cells may be unable to polarize in isolation and depend on cell-cell signals (e.g., fluxes or gradients between cells) to both establish and coordinate polarity [7–10]. A further question is the relationship between cell polarity and growth. Polarity may guide growth orientation [11], and/or differential cell wall loosening may orient polarity [9].

One way of addressing these questions is to study the localization of polarity proteins in cell cultures or protoplasts where cell neighbors can be reduced or eliminated. Expression of polarity proteins PIN1 (auxin transporter) and BOR1 (borate transporter) in tobacco BY-2 cell filaments gives signal at cross-walls between cells but no obvious polarity from one end of the cell to the other, except for terminal cells, which have only one cross-wall [12–18]. In protoplasts, PIN and SOSEKI do not exhibit polarity [1, 14, 19], and it has been proposed that PIN polarity is maintained though association with domains connected to the cell wall, preventing lateral diffusion [20]. Thus, so far there is no clear evidence for intrinsic polarity.

Here, we analyze the behavior of another polarity protein, BASL. BASL is polarly localized in stomatal lineages of *Arabidopsis*, where it plays a role in controlling asymmetric cell divisions [21, 22]. Localization of BASL and its interactor, BRXL2, is biased toward the proximal end of stomatal lineage cells (i.e., end toward the leaf base) suggesting it responds to a tissue-wide pattern [23, 24]. This proximal bias is further highlighted through ectopic expression of BASL. Induction experiments suggest proximal localization of ectopic BASL depends on its interaction with other proteins or complexes at one end of the cell, constituting a polarized molecular address [24]. Ectopic BASL exhibits polarity reversals at serrations, similar to that observed with PINs, suggesting that BASL and PIN polarity patterns interact. Thus, BASL localization reveals coordinated tissue cell polarity in both endogenous and ectopic contexts.

BASL Is Polarly Localized in Tobacco BY-2 Cells

To test whether BASL may be polarly localized in BY-2 cells, we performed transient expression assays by incubating a BY-2 culture with Agrobacterium harboring either 35S::GFP-BASL or 35S::GFP as a control. BY-2 filaments expressing

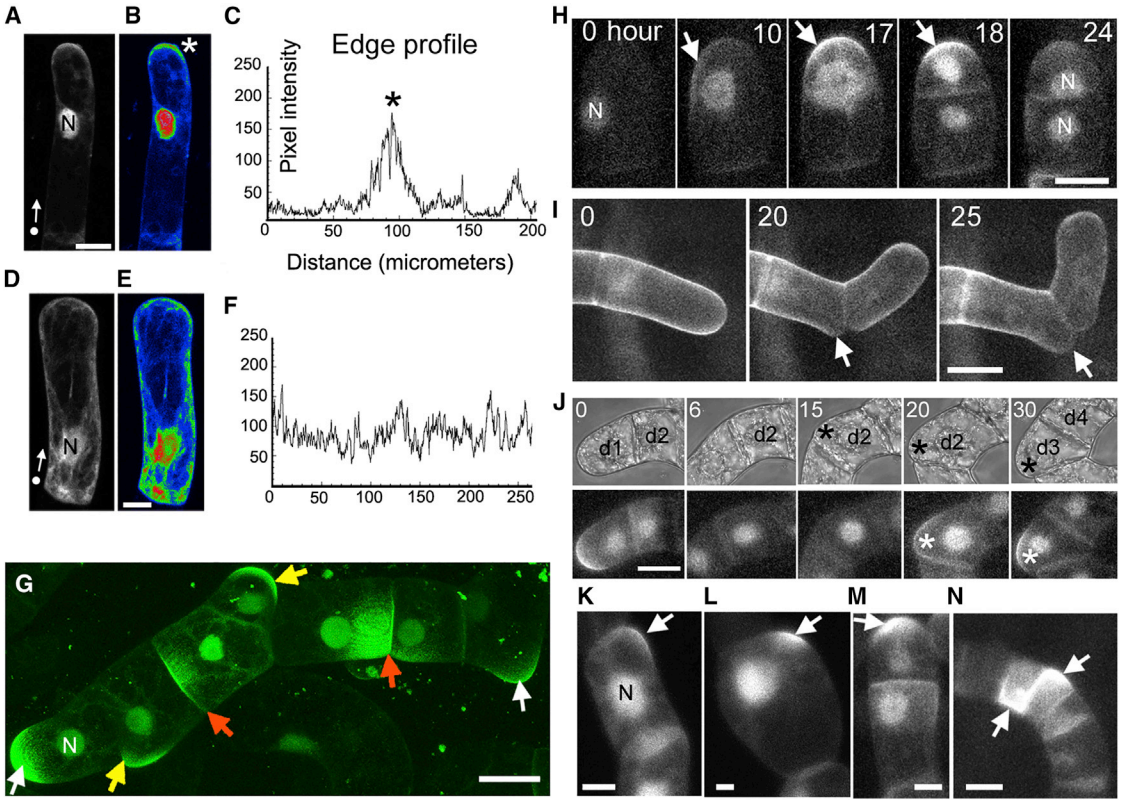

Figure 1. Ectopic BASL Is Polarized in BY-2 Cells

(A–F) (A) BY-2 cell transformed with GFP-BASL in transient assay. (B) Same cells as in (A) with pixel intensities labeled using Rainbow RGB lookup table. The asterisk marks polarized BASL. (C) Cell perimeter intensity profile of cell shown in (A). The intensity profile was plotted from the dot shown in (A) around the perimeter of the cell in the direction indicated by the arrow (i.e., the left-hand side of edge profiles corresponds to the position of the dot). (D) BY-2 cell transformed with soluble GFP. (E) Same cell as in (D) with pixel intensities labeled using Rainbow RGB lookup table. (F) Edge intensity profile of cell shown in (D). The dot and arrow in (A) and (D) mark the origin and direction of the edge intensity profile, respectively.

(G) Filaments of transgenic BY-2 culture transformed with 35S::GFP-BASL. Polarized BASL observed at filament ends (white arrows), internal walls (red arrows), and bulges (yellow arrows). BASL signal is also detected in nuclei (N).

(H) Polarized BASL (arrows) appears before (t = 10) and disappears after (t = 24) cell division. The fluorescence intensity of polarized and nuclear GFP-BASL increases as the cell approaches cell division.Cell division occurs at about 17 h.

(I) Untransformed BY-2 cells showing formation of bulges at sites of filament fragmentation (arrow). Cell wall stained with Direct Fast Red B.

(J) Development of fragmentation site in daughter cell shown in light field (upper panel) or fluorescence labeling with GFP-BASL (lower panel). Terminal cell of filament divides giving rise to a daughter cell with (d1, 0 h) and without polarized BASL (d2). The corner of cell d2 develops a bulge (black asterisk). Polarized BASL appears strongly at the bulge (white asterisk) before the d2 cell divides giving rise to cells d3 and d4 (20 h).

(K and L) Polarized BASL observed in cell cultures grown in 10 μM oryzalin after 30 (K) and 80 (L) h. Cells swell after 80 h. Arrows indicate polarized BASL.

(M and N) Polarized BASL observed in cell cultures grown in 250 nM latrunculin for 27 (M) and 62 (N) h. Cell division gives rise to small cells after 62 h. Arrows indicate polarized BASL.

Scale bars (A), (E), and (G): 15 μm; (H), (I), and (J): 30 μm; (K–N): 20 μm. Time (H) and (I) = hours. t = 0 in (H), (I), and (J) refers to 0, 12, and 6 h after starting imaging, respectively. See also Figures S1, S2, and S3.

35S::GFP-BASL often displayed a cortical patch of fluorescence at their tips, forming an intensity peak in cell-perimeter profiles (Figures 1A–1C; Figures S1A–S1L). Such patches were not observed in controls expressing 35S::GFP (Figures 1D–1F; Figures S1M–S1X). For both 35S::GFP-BASL and 35S::GFP, signal was also observed in the nucleus. The localization pattern for 35S::GFP was consistent with other BY-2 cell studies [25, 26]. Close BASL homologs are restricted to relatives of *Arabidopsis* [27] (we found the nearest homolog in tobacco has 35% amino acid identity). Our results suggest that ectopic BASL may nevertheless be attracted to a conserved polarized molecular address in tobacco BY-2 cells.

To follow ectopic BASL polarity during growth of BY-2 filaments, we created a stably transformed 35S::GFP-BASL line. In transgenic 35S::GFP-BASL, signal was observed in the nucleus and at a range of polarized locations: the tip of the filament (white arrows, Figure 1G), at or near cell junctions (red arrows), toward side walls, and at lateral bulges (yellow arrows).

The intensity of polarized BASL signal at the filament tip or other locations (including the nucleus) increased as cells approached division (Figure 1H). BASL signal also appeared transiently at the cell plate. Nuclear position was not strongly biased by polarized BASL prior to cell division (Figures S2A–S2D). Two types of daughter cells were produced after cell division: one

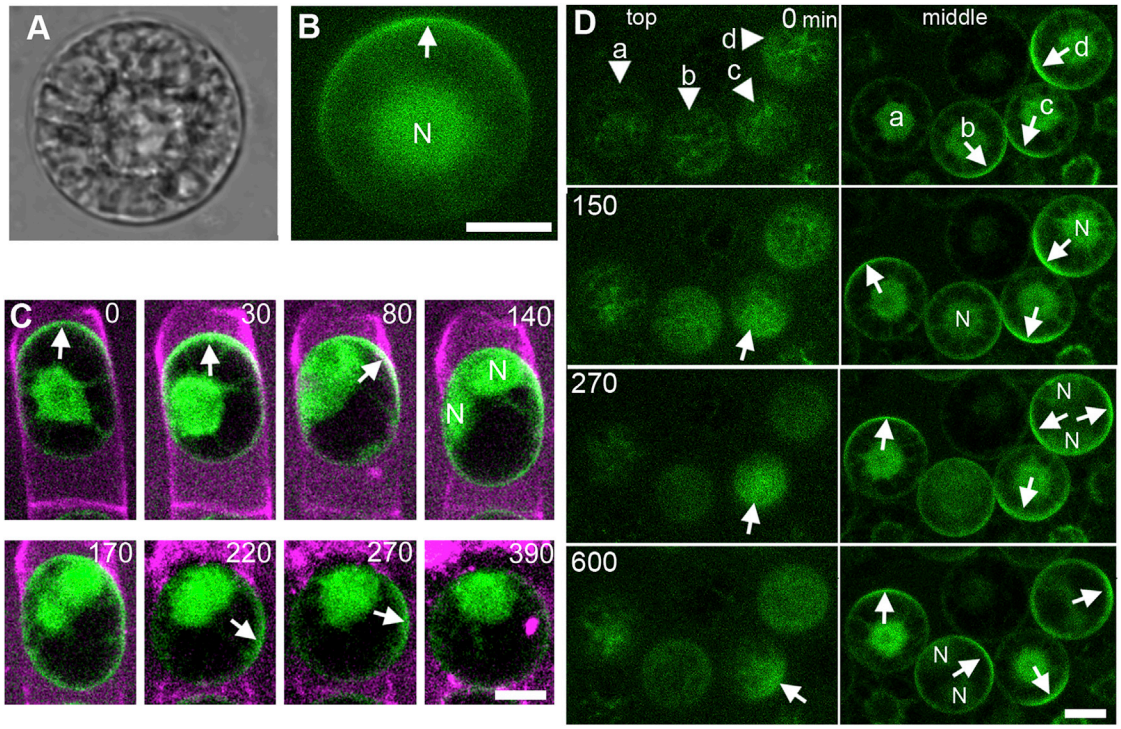

Figure 2. BASL Is Polarized in Protoplasts

(A) Light field view of protoplast after 3 h in protoplasting solution.

(B) Distribution of GFP-BASL in the same protoplast as (A).

(C) Formation of protoplast. First time point (0 min) taken a few minutes after addition of protoplasting solution. Nuclear division between 80 min and 140 min (no cell wall forms as the cells are in protoplasting solution). Magenta = cell wall stained with Direct Fast Red B.

(D) Polarized BASL is dynamic and not coordinated in protoplasts. Z-slices taken from the top (left column) or middle (right column) plane of protoplasts at different times. In protoplast (a), polarized BASL appears on the side face of (middle, 150 min). In protoplast (b), polarized BASL disappears from the side face (middle, 150 min) and reappears in a new location (middle, 600 min). In protoplast (c), polarized BASL moves from side to top face (top, 270 min). In protoplast (d), a transition with two foci of polarized BASL occurs. The side face locations of polarized BASL changes after cell division in protoplasts (b) and (d). Arrows indicates polarized BASL; N, nucleus.

Scale bars (A–C): 15 μm; (D): 20 μm. Time (C) and (D) = min. See also Videos S1 and S2; Figure S4.

without polarized BASL and the other containing the parental patch, which was lost shortly afterward. Polarized BASL could appear in both types of daughter cells later during their cell cycle. Polarized BASL appeared on average 11 h before cell division (n = 18, SD = 4 h) and was evident during 44% (SD = 13%) of the cell cycle (mean cycle duration 27 h, SD = 11 h). Thus, ectopic BASL is polarly localized in BY-2 cultures, with timing and intensity linked to the cell cycle. Cell-cycle dependency is also observed for endogenous BASL in *Arabidopsis* [21, 22], indicating that elements of this coupling are preserved in the BY-2 context.

The observation of BASL signal at lateral bulges of BY-2 filaments is reminiscent of outgrowths seen on epidermal cells when BASL is expressed ectopically in plants [21], which could suggest that ectopic BASL induces these bulges. However, untransformed BY-2 cells also exhibited lateral bulges at positions where filaments eventually fragment and form new tips (Figure 1I). The number of fragmentation sites was not significantly different between transformed and untransformed cultures (two replicates; Figures S2E and S2F). Moreover, BASL typically appeared at lateral bulges after they had formed (Figure 1J; Figure S3). Thus, rather than ectopic BASL promoting formation of bulges in BY-2 filaments, BASL likely interacts with proteins that accumulate at sites of cell fragmentation, constituting presumptive tip addresses.

To determine whether polarized GFP-BASL was dependent on cytoskeletal components, transgenic BY-2 cultures were incubated for several days with either oryzalin (a microtubule polymerization inhibitor) or latrunculin (an actin polymerization inhibitor). BASL was polarly localized during both treatments (despite cells displaying abnormal growth and division), showing that neither actin nor microtubules are likely required for asymmetric localization (Figures 1K–1N). This lack of dependence on cytoskeletal components is similar to that observed for BASL and other polarity proteins (PINs and SOSEKIs) in *Arabidopsis* [1, 9, 14, 23, 24, 28].

BASL Is Polarly Localized in Protoplasts

To determine whether BASL can become polarized in the absence of cell neighbors or a cell wall, BY-2 cells expressing ectopic BASL were treated with cellulase and pectolyase to generate protoplasts. Spherical protoplasts could be observed 3 h after treatment. About 16% of these protoplasts (6/39, 6/26, 9/55, 8/69 in four replicates) exhibited polarly localized

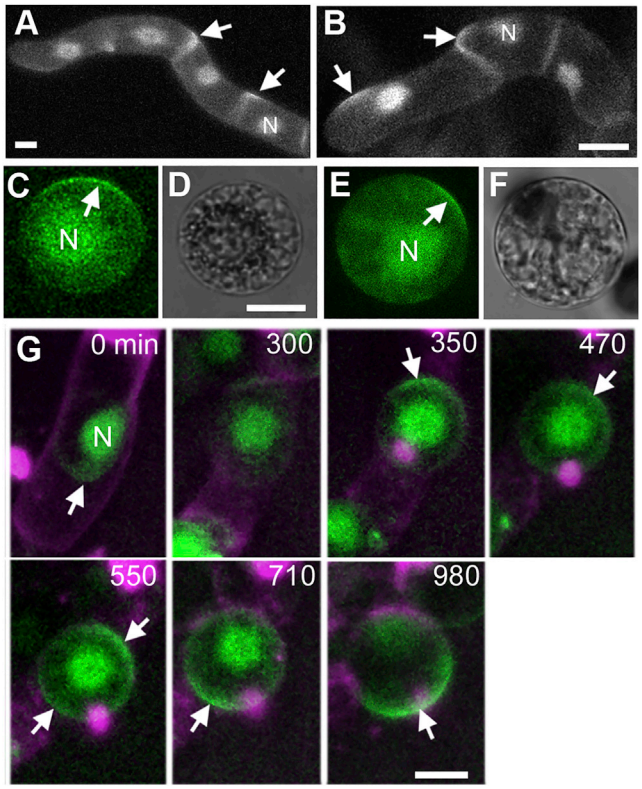

Figure 3. BASL Is Polarized in the Presence of Auxin Transport Inhibitors

(A and B) Polarized BASL observed in cell cultures grown in 50 μM NPA for 20 (A) and 40 (B) h.

(C) Protoplast formed in presence of 50 μm NPA from BY-2 cells cultured in NPA for 24 h. White arrow indicates polarized BASL.

(D) Bright field image of (C).

(E) Protoplast formed in the presence of 5 μm TIBA from BY-2 cells cultured in TIBA for 24 h. White arrow indicates polarized BASL.

(F) Bright field image of (E). N, nucleus.

(G) Dynamics of polarized GFP-BASL in an NPA-treated cell becoming a protoplast. Polarized GFP-BASL is first located at the bottom side of the cell (0 min) and then changes location twice as the cell becomes spherical: first from the lower to the upper side (350 min) and then from the upper to the lower side of the protoplast (710 min). A transitional state occurs in which polarized GFP-BASL forms two caps (550 min). Four cells were filmed turning into protoplasts. In three of these cells, polarized BASL disappeared and appeared in a new location either before (two cells) or after becoming spherical. In one of the cells, no polarized BASL was evident at the start of the movie, and polarized BASL appeared after it became spherical. Two cells underwent nuclear division before polarity appeared.

Scale bars (A), (C), (D), and (G): 20 μm; (B): 30 μm; (E) and (F): 10 μm.

BASL (Figures 2A and 2B). 3D projections revealed polarized BASL formed a cap (Video S1), which was estimated to occupy about 18% (n = 35; see Method Details) of the area of the spherical protoplast.

To quantify BASL polarity, we performed ratiometric analysis using the membrane stain FM4-64 as a control. FM4-64 displayed two peaks of fluorescence in protoplasts, located at opposite ends of the cell (Figure S4A). The orientation of the peaks did not change as the specimen was rotated, showing that the pattern was caused by photoselective excitation of the FM4-64 stain rather than its selective localization (Figures S4A, S4B, and S4D). By contrast, ectopic BASL gave a single peak of fluorescence that rotated together with the cell (Figures S4A, S4C, and S4E). The fluorescence ratio in regions where polarized BASL and FM4-64 colocalized revealed that GFP signal was on average 3.2-fold greater (n = 10, SD = 1.2, two replicates) in the domain with polarized BASL compared to that at the opposite end.

BASL Polarity Is Dynamic in Protoplasts

To determine whether BASL polarity in protoplasts reflected carryover from parental cells of the filament, we filmed BASL localization during formation of seven protoplasts. In two cases, polarized BASL disappeared as protoplasts formed, and in one of these cases, it then reappeared in new locations following nuclear division (Figure 2C; Video S2 [Part 1]; note that in protoplasting solution, nuclei divide without formation of a new cell wall). In the remaining five cases, polarized BASL was initially not detected and then appeared during protoplast formation (e.g., Figure S4F; Video S2 [Part 2]). It either appeared while cells were becoming spherical (two cases; Figure S4F; Video S2 [part 2]) or afterward (3 cases). Thus, BASL polarity can be established during or after protoplast formation in locations distinct from those in the progenitor filament.

The long-term behavior of polarized BASL was filmed for eight protoplasts after they had formed. In five cases, polarized BASL remained relatively static (e.g., Figure 2D, protoplast a; Figure S4G) prior to division, whereas in three, it changed location (e.g., Figure 2D, protoplast c). Seven protoplasts underwent nuclear division while being filmed, and in all cases, polarized BASL disappeared before division and then reappeared in a new location after division into two nuclei. It then disappeared shortly afterward, when the daughter nuclei fused (average duration after reappearance was 130 min, SD = 25 min; e.g., Figure 2D, protoplasts d and b; Figure S4G). In five cases, a transition state with polarized BASL at two locations was observed (before or after division), demonstrating that shifts in location were not due to protoplast rotation but rather the generation of new localization sites. BASL polarity was not strongly coordinated between protoplasts (Figure S4H).

BASL Polarity Is Resistant to Auxin Transport Inhibitors

Given the parallels between ectopic BASL and PIN localization in developing leaves [24], we tested whether BASL polarity in BY-2 cells depended on auxin transport. Treating cells with the auxin transport inhibitor NPA did not obviously perturb the behavior of polarized GFP-BASL in cellular filaments (Figures 3A and 3B) or protoplasts (Figures 3C and 3D). Like untreated controls (Figure 2C), the location of polarized GFP-BASL could shift during and after protoplasting (Figure 3G). Treating filaments or protoplasts with a different auxin transport inhibitor, TIBA, yielded a similar BASL polarity pattern to untreated controls (Figures 3E and 3F). Thus, BASL could exhibit dynamic polar localization in protoplasts in the presence of auxin transport inhibitors.

BASL Polarity Aligns with the Growth Axis during Protoplast Regeneration

Placing protoplasts in regeneration medium allows cell wall formation followed by elongation to form a sausage-shaped cell [29]. To see how polarized BASL relates to the growth axis, we measured the aspect ratio (major axis/minor axis) of 60 cells

one day after regeneration and determined their pattern of BASL localization. Forty cells had low aspect ratios (1.1 to 1.5), and BASL showed no significant preference for localization to a long or short side of the cell (22 and 18, respectively; $p = 0.527$; Figures S4I–S4N). The remaining 20 cells had higher aspect ratios (1.6 to 3.2). For 19 of these, polarized BASL was found only on a short side, demonstrating significant bias for short versus long ($p = 0.00006$) (Figures S4O–S4R). The cell with BASL on a long side also had a second patch of BASL on a short side (Figure S4S). Thus, in elongated cells, BASL localizes preferentially to a short end, and its polarity is therefore aligned with the cell's long axis.

To determine how polarity alignment arises, we live-imaged six regenerating protoplasts. Three showed no strong divergence between minor and major axis lengths over time (i.e., did not elongate; Figures 4M–4O) and exhibited dynamic BASL behavior (Figure 4, protoplasts A, C, and E; Video S3). The other three cells developed a clear axis of anisotropic growth (Figures 4P–4U), with growth becoming largely restricted to the major axis (Figure 4, protoplasts G, I, and K). In these cells, BASL polarity became fixed at one end of the axis. In some cases, diffuse polarized BASL anticipated the growth axis (Figure 4, protoplast G; Video S4 [Part 1]), whereas in others, BASL polarity was concomitant with (Figure 4, protoplast I; Video S4 [Part 2]) or appeared shortly after (Figure 4, protoplast K) growth anisotropy became evident. The polarity revealed by ectopic BASL precedes asymmetric nuclear positioning, which occurs after the cell has acquired an ovoid shape [29]. Thus, BASL polarity is aligned with the growth axis around the time anisotropy becomes evident, whereas it remains dynamic in isotropically growing cells.

Conclusions

We show that BASL can become asymmetrically localized when ectopically expressed in cell culture, most likely marking an endogenous polarized molecular address. Polarity can be established in the absence of neighbors, in spherical cells that lack obvious mechanical asymmetries, and in the presence of auxin transport inhibitors or drugs that inhibit actin or microtubule polymerization. Moreover, polarity is dynamic, suggesting it may be steerable through cues. These findings are consistent with models in which cell polarity is established through a cell-intrinsic mechanism, with intercellular cues serving to coordinate this polarity between cells.

In contrast to ectopic BASL, PIN and SOSEKI polarity proteins do not exhibit polarized localization in protoplasts [1, 14, 19]. This may reflect the absence of polarity addresses for these proteins or the inability of these proteins to interact with addresses in this context. It is also possible that for these proteins, extrinsic cues are needed to establish as well as coordinate polarity.

We further show that ectopic BASL polarity is modulated during the cell cycle and is aligned with the growth axis around the time the axis becomes evident in regenerating protoplasts. Studies with regenerating moss protoplasts have shown that a growth axis can be fixed in random orientations in the absence of external cues [30]. Transient exposure to cues (e.g., light) in moss and algae demonstrates that alignment of this axis with the cue precedes anisotropic growth by several hours [30, 31]. Unlike axial growth of BY-2 cells, growth is polarized in these cases, creating a protrusion at one end of the cell, and thus a pear shape rather than an ovoid. Fixation of this growth polarity (i.e., which end of the axis produces the outgrowth) with regard to the cue occurs after alignment of the growth axis [30].

Taken together with our results, these findings suggest the following working hypothesis. In the absence of external cues, regenerating protoplasts contain an intrinsic polarized molecular address that can vary in position over time. If this position continues to vary, cells grow isotropically. However, the address may spontaneously become fixed in a random orientation. The axial orientation defined by this polarity may lead to a bias in cell wall properties and thus anisotropic growth. The change in cell shape brought about by anisotropic growth may also reinforce the localization of the polarized address. Ectopic BASL labels the polarized address for about 45% of the cell cycle and may therefore highlight the address prior to or during growth anisotropy. External cues can modify this process by biasing the orientation of the polarized molecular address. In cases of polarized outgrowth, such as regenerating moss protoplasts, prolonged exposure to the cue may also be needed to fix the end of the cell from which outgrowth occurs.

In a multicellular tissue, similar processes may underlie the observed coupling between cell polarity and the orientation of growth, with developmental signals providing orienting cues in this case [6]. Elements of this process may be evident in BY-2 filaments, where ectopic BASL often marks growth axes by being localized at tips or fragmentation sites. Additional evidence for polarized molecular addresses playing a role in multicellular tissues comes from experiments in which PIN proteins can be redirected to different ends of root cells by modifying their amino acid sequence [32] and from the demonstration that SOSEKIs, phylogenetically ancient polarity proteins, can recruit other proteins to polarized locations [33]. Further experiments are needed to establish the relationship between polarity, axiality, and remodeling of the cytoskeleton and cell wall during protoplast regeneration and to fully characterize components of polarized molecular addresses.

STAR★METHODS

Detailed methods are provided in the online version of this paper and include the following:

- KEY RESOURCES TABLE
- RESOURCE AVAILABILITY
  - Lead Contact
  - Materials Availability
  - Data and Code Availability
- EXPERIMENTAL MODEL AND SUBJECT DETAILS
  - Growth conditions
- METHOD DETAILS
  - Generation of BY2 cells containing 35S::GFP-BASL and 35S::GFP
  - Drug treatments
  - Labeling of cell walls
  - Formation of protoplasts
  - FM4-64 labeling of protoplasts
  - Protoplast regeneration
  - Microscopy
- QUANTIFICATION AND STATISTICAL ANALYSIS

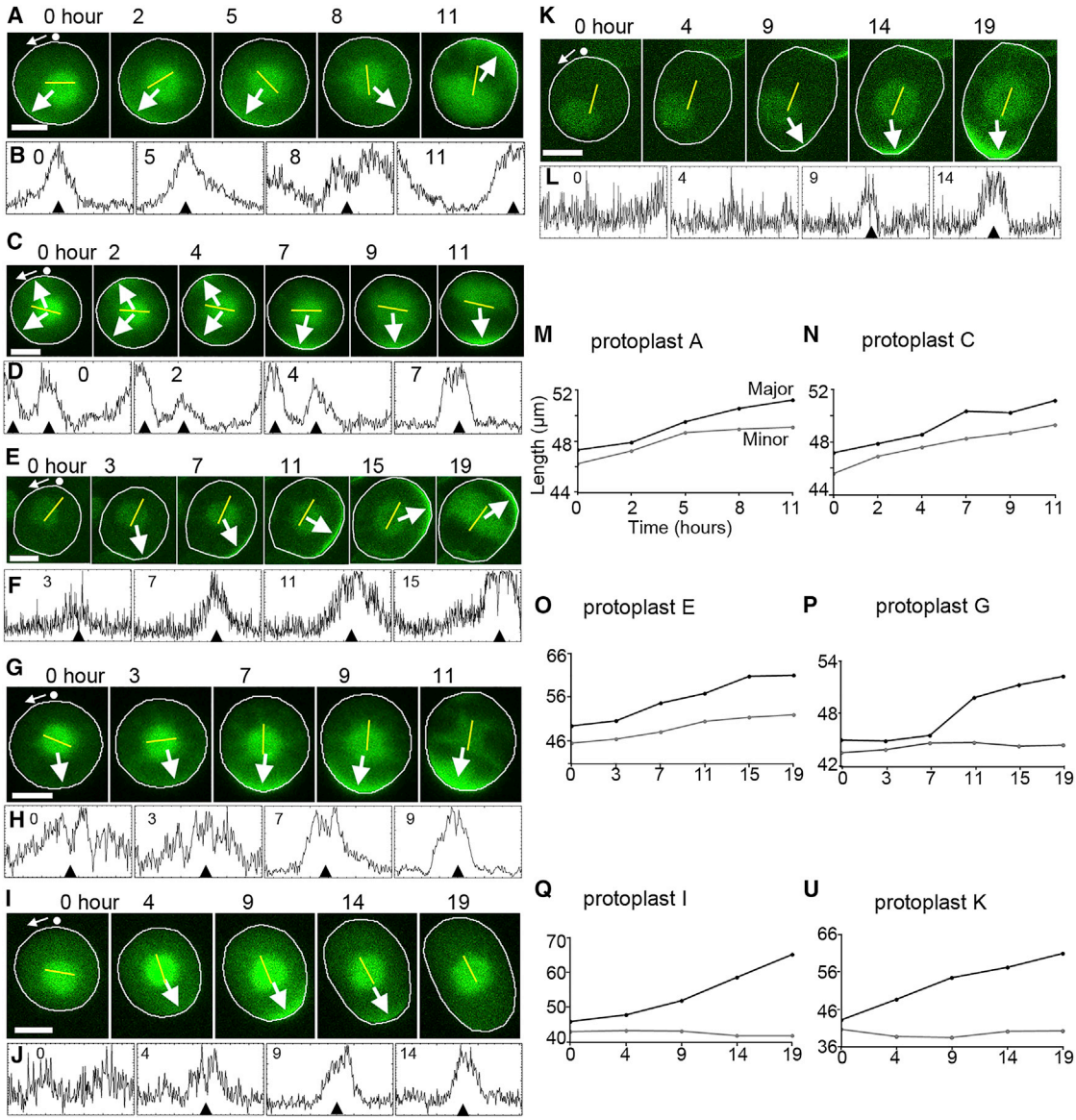

Figure 4. Dynamics of Polarized BASL in Regenerating Protoplasts Reflect Growth Axis

(A, C, and E) Dynamics of polarized BASL in isotropically growing regenerating protoplasts. Protoplast A, polarized BASL changes orientation from 7 o'clock (t = 0) to 4 o'clock (t = 8) and then to 1 o'clock (t = 11). The orientation of the major axis varies during regeneration until 8 h. There is no strong divergence between minor and major axis lengths (M). Protoplast C, two caps of polarized BASL (t = 0–4) become a single cap at 6 o'clock (t = 7–11). The orientation of the major axis is relatively fixed. There is no strong divergence between minor and major axis lengths (N). Protoplast E, polarized BASL appears at 5 o'clock at t = 7 and then progressively changes orientation to 1 o'clock (t = 7–19). The orientation of the major axis is relatively fixed. There is no strong divergence between minor and major axis lengths (O). (B, D, and F) Corresponding edge profiles of isotropically growing protoplasts at selected times. The black arrow heads indicate the positions marked by the arrows in the microscopy images. (G, I, and K) Dynamics of polarized BASL in anisotropically growing protoplasts. Protoplast G, BASL is diffusely polarized at t = 0 (J) and then becomes strongly polarized at t = 7 (J) just before anistropic growth becomes evident (P). The major axis also becomes fixed at t = 7. Protoplast I, polarized BASL appears at t = 4 and then disappears after 19 h. Growth is largely restricted to the major axis (Q). Protoplast K, polarized BASL appears at t = 4. Growth is largely restricted to the major axis (U). (H, J, and L) Edge profiles of anisotropically growing protoplasts at selected times. (M–U) Major and minor axis of protoplasts shown in (A), (C), (E), (G), (I), and (K). White arrows and black arrowheads indicate polarized BASL. Yellow line indicates orientation of the major axis (the length of the line is fixed and does not indicate the magnitude of the differential between major and minimum axes). N, nucleus.

Scale bars (A), (C), (E), (G), (I), (K), and (M): 20 μm. Time zero refers to when imaging was started, which was 1–2 h after cells were transferred into regeneration media. The data were obtained from four independent experiments. See also Videos S3 and S4.

SUPPLEMENTAL INFORMATION

Supplemental Information can be found online at https://doi.org/10.1016/j.cub.2020.09.036.

ACKNOWLEDGMENTS

We thank JIC Bioimaging, Laboratory support for supplying media. We also thank Christine Faulkner for providing the 35S::EGFP-nos construct and Desmond Bradley, Chris Whitewoods, and Beatriz Pinto-Goncalves for their feedback on the manuscript. The work was supported by grants from Biotechnology and Biological Sciences Research Council, UK: BB/L008920/1, BBS/E/J/00000152, BB/F005997/1, and BBS/E/J/000PR9787.

AUTHOR CONTRIBUTIONS

J.C., C.M., F.C., D.D., and E.C. conceived and designed the study. J.C., C.M., F.C., and D.D. acquired data and developed resources. E.C. and J.C. provided supervision. J.C. and E.C. wrote the manuscript. All authors reviewed and revised the manuscript.

DECLARATION OF INTERESTS

The authors declare no competing interests.

Received: January 22, 2020
Revised: August 7, 2020
Accepted: September 11, 2020
Published: October 8, 2020

REFERENCES

1. Yoshida, S., van der Schuren, A., van Dop, M., van Galen, L., Saiga, S., Adibi, M., Möller, B., Ten Hove, C.A., Marhavy, P., Smith, R., et al. (2019). A SOSEKI-based coordinate system interprets global polarity cues in Arabidopsis. Nat. Plants *5*, 160–166.
2. Lee, L.R., and Bergmann, D.C. (2019). The plant stomatal lineage at a glance. J. Cell Sci. *132*, jcs228551.
3. Biedroń, M., and Banasiak, A. (2018). Auxin-mediated regulation of vascular patterning in Arabidopsis thaliana leaves. Plant Cell Rep. *37*, 1215–1229.
4. Traas, J. (2013). Phyllotaxis. Development *140*, 249–253.
5. Coen, E., Kennaway, R., and Whitewoods, C. (2017). On genes and form. Development *144*, 4203–4213.
6. Abley, K., De Reuille, P.B., Strutt, D., Bangham, A., Prusinkiewicz, P., Marée, A.F., Grieneisen, V.A., and Coen, E. (2013). An intracellular partitioning-based framework for tissue cell polarity in plants and animals. Development *140*, 2061–2074.
7. Jönsson, H., Heisler, M.G., Shapiro, B.E., Meyerowitz, E.M., and Mjolsness, E. (2006). An auxin-driven polarized transport model for phyllotaxis. Proc. Natl. Acad. Sci. USA *103*, 1633–1638.
8. Smith, R.S., Guyomarc'h, S., Mandel, T., Reinhardt, D., Kuhlemeier, C., and Prusinkiewicz, P. (2006). A plausible model of phyllotaxis. Proc. Natl. Acad. Sci. USA *103*, 1301–1306.
9. Heisler, M.G., Hamant, O., Krupinski, P., Uyttewaal, M., Ohno, C., Jönsson, H., Traas, J., and Meyerowitz, E.M. (2010). Alignment between PIN1 polarity and microtubule orientation in the shoot apical meristem reveals a tight coupling between morphogenesis and auxin transport. PLoS Biol. *8*, e1000516.
10. Bayer, E.M., Smith, R.S., Mandel, T., Nakayama, N., Sauer, M., Prusinkiewicz, P., and Kuhlemeier, C. (2009). Integration of transport-based models for phyllotaxis and midvein formation. Genes Dev. *23*, 373–384.
11. Whitewoods, C.D., Gonçalves, B., Cheng, J., Cui, M., Kennaway, R., Lee, K., Bushell, C., Yu, M., Piao, C., and Coen, E. (2020). Evolution of carnivorous traps from planar leaves through simple shifts in gene expression. Science *367*, 91–96.
12. Maisch, J., Fiserová, J., Fischer, L., and Nick, P. (2009). Tobacco Arp3 is localized to actin-nucleating sites in vivo. J. Exp. Bot. *60*, 603–614.
13. Yamauchi, N., Gosho, T., Asatuma, S., Toyooka, K., Fujiwara, T., and Matsuoka, K. (2013). Polarized localization and borate-dependent degradation of the Arabidopsis borate transporter BOR1 in tobacco BY-2 cells. F1000Res. *2*, 185.
14. Boutté, Y., Crosnier, M.T., Carraro, N., Traas, J., and Satiat-Jeunemaitre, B. (2006). The plasma membrane recycling pathway and cell polarity in plants: studies on PIN proteins. J. Cell Sci. *119*, 1255–1265.
15. Jelínková, A., Malínská, K., Simon, S., Kleine-Vehn, J., Parezová, M., Pejchar, P., Kubes, M., Martinec, J., Friml, J., Zazímalová, E., and Petrásek, J. (2010). Probing plant membranes with FM dyes: tracking, dragging or blocking? Plant J. *61*, 883–892.
16. Dhonukshe, P., Grigoriev, I., Fischer, R., Tominaga, M., Robinson, D.G., Hasek, J., Paciorek, T., Petrásek, J., Seifertová, D., Tejos, R., et al. (2008). Auxin transport inhibitors impair vesicle motility and actin cytoskeleton dynamics in diverse eukaryotes. Proc. Natl. Acad. Sci. USA *105*, 4489–4494.
17. Aubert, A., Marion, J., Boulogne, C., Bourge, M., Abreu, S., Bellec, Y., Faure, J.D., and Satiat-Jeunemaitre, B. (2011). Sphingolipids involvement in plant endomembrane differentiation: the BY2 case. Plant J. *65*, 958–971.
18. Müller, K., Hošek, P., Laňková, M., Vosolsobě, S., Malínská, K., Čarná, M., Fílová, M., Dobrev, P.I., Helusová, M., Hoyerová, K., and Petrášek, J. (2019). Transcription of specific auxin efflux and influx carriers drives auxin homeostasis in tobacco cells. Plant J. *100*, 627–640.
19. Dory, M., Hatzimasoura, E., Kállai, B.M., Nagy, S.K., Jäger, K., Darula, Z., Nádai, T.V., Mészáros, T., López-Juez, E., Barnabás, B., et al. (2018). Coevolving MAPK and PID phosphosites indicate an ancient environmental control of PIN auxin transporters in land plants. FEBS Lett. *592*, 89–102.
20. Feraru, E., Feraru, M.I., Kleine-Vehn, J., Martinière, A., Mouille, G., Vanneste, S., Vernhettes, S., Runions, J., and Friml, J. (2011). PIN polarity maintenance by the cell wall in Arabidopsis. Curr. Biol. *21*, 338–343.
21. Dong, J., MacAlister, C.A., and Bergmann, D.C. (2009). BASL controls asymmetric cell division in Arabidopsis. Cell *137*, 1320–1330.
22. Robinson, S., Barbier de Reuille, P., Chan, J., Bergmann, D., Prusinkiewicz, P., and Coen, E. (2011). Generation of spatial patterns through cell polarity switching. Science *333*, 1436–1440.
23. Bringmann, M., and Bergmann, D.C. (2017). Tissue-wide Mechanical Forces Influence the Polarity of Stomatal Stem Cells in Arabidopsis. Curr. Biol. *27*, 877–883.
24. Mansfield, C., Newman, J.L., Olsson, T.S.G., Hartley, M., Chan, J., and Coen, E. (2018). Ectopic BASL Reveals Tissue Cell Polarity throughout Leaf Development in Arabidopsis thaliana. Curr. Biol. *28*, 2638–2646.e4.
25. Koroleva, O.A., Tomlinson, M.L., Leader, D., Shaw, P., and Doonan, J.H. (2005). High-throughput protein localization in Arabidopsis using Agrobacterium-mediated transient expression of GFP-ORF fusions. Plant J. *41*, 162–174.
26. van Leeuwen, W., Vermeer, J.E., Gadella, T.W., Jr., and Munnik, T. (2007). Visualization of phosphatidylinositol 4,5-bisphosphate in the plasma membrane of suspension-cultured tobacco BY-2 cells and whole Arabidopsis seedlings. Plant J. *52*, 1014–1026.
27. Vatén, A., and Bergmann, D.C. (2012). Mechanisms of stomatal development: an evolutionary view. Evodevo *3*, 11.
28. Geldner, N., Friml, J., Stierhof, Y.D., Jürgens, G., and Palme, K. (2001). Auxin transport inhibitors block PIN1 cycling and vesicle trafficking. Nature *413*, 425–428.
29. Zaban, B., Maisch, J., and Nick, P. (2013). Dynamic actin controls polarity induction de novo in protoplasts. J. Integr. Plant Biol. *55*, 142–159.
30. Cove, D.J., Quatrano, R.S., and Hartmann, E. (1996). The alignment of the axis of asymmetry in regenerating protoplasts of the moss, Ceratodon

purpureus, is determined independently of axis polarity. Development *122*, 371–379.

31. Quatrano, R., and Shaw, S. (1997). Role of the cell wall in the determination of cell polarity and the plane of cell division in Fucus embryos. Trends Plant Sci. *2*, 15–21.
32. Zhang, J., Nodzynski, T., Pencík, A., Rolcík, J., and Friml, J. (2010). PIN phosphorylation is sufficient to mediate PIN polarity and direct auxin transport. Proc. Natl. Acad. Sci. USA *107*, 918–922.
33. van Dop, M., Fiedler, M., Mutte, S., de Keijzer, J., Olijslager, L., Albrecht, C., Liao, C.Y., Janson, M.E., Bienz, M., and Weijers, D. (2020). DIX Domain Polymerization Drives Assembly of Plant Cell Polarity Complexes. Cell *180*, 427–439.e12.
34. Thomas, C.L., Bayer, E.M., Ritzenthaler, C., Fernandez-Calvino, L., and Maule, A.J. (2008). Specific targeting of a plasmodesmal protein affecting cell-to-cell communication. PLoS Biol. *6*, e7.
35. Weber, E., Gruetzner, R., Werner, S., Engler, C., and Marillonnet, S. (2011). Assembly of designer TAL effectors by Golden Gate cloning. PLoS ONE *6*, e19722.
36. Buschmann, H., Green, P., Sambade, A., Doonan, J.H., and Lloyd, C.W. (2011). Cytoskeletal dynamics in interphase, mitosis and cytokinesis analysed through Agrobacterium-mediated transient transformation of tobacco BY-2 cells. New Phytol. *190*, 258–267.
37. Chan, J., Crowell, E., Eder, M., Calder, G., Bunnewell, S., Findlay, K., Vernhettes, S., Höfte, H., and Lloyd, C. (2010). The rotation of cellulose synthase trajectories is microtubule dependent and influences the texture of epidermal cell walls in Arabidopsis hypocotyls. J. Cell Sci. *123*, 3490–3495.
38. Calder, G., Hindle, C., Chan, J., and Shaw, P. (2015). An optical imaging chamber for viewing living plant cells and tissues at high resolution for extended periods. Plant Methods *11*, 22.

STAR★METHODS

KEY RESOURCES TABLE

REAGENT or RESOURCE	SOURCE	IDENTIFIER
Chemicals, Peptides, and Recombinant Proteins		
Oryzalin	Sigma-Aldridge	Cat#36182
Latruculin	Abcam	Cat#144291
Naphthalenacetic acid	Sigma-Aldridge	Cat#N1641
Benzylaminopurine	Sigma-Aldridge	Cat#B3274
Direct Fast Red B	Sigma-Aldridge	Cat#R314188
Cellulase "Onozuka" R-10	Yakult Pharmaceutical	N/A
Pectolyase Y23	Duchefa Biochemie	Cat#P8004.0001
FM4-64	Invitrogen	Cat#T3166
Experimental Models: Organisms/Strains		
BY-2 cells containing GFP-BASL	This paper	available on request
Recombinant DNA		
35S::GFP-BASL-Act-2 construct	This paper	available on request
35S::EGFP-Nos construct	[34]	N/A
Software and Algorithms		
ImageJ	freely available	ImageJ https://imagej.nih.gov/ij/
Chi-square goodness of fit tests	freely available	http://quantpsy.org/chisq/chisq.htm

RESOURCE AVAILABILITY

Lead Contact

Further information and requests for plant lines, constructs and raw data should be directed to and will be fulfilled by the Lead Contact, Enrico Coen (enrico.coen@jic.ac.uk).

Materials Availability

This study did not generate new unique reagents.

Data and Code Availability

This study did not generate any unique code. Data are available at https://figshare.com/s/9e5c5de33b8d0db03a94.

EXPERIMENTAL MODEL AND SUBJECT DETAILS

Either untransformed suspension cultures of *Nicotiana tabacum* Bright Yellow-2 (BY-2) cells or cells transformed with 35S::GFP-BASL or 35S::GFP were used for experiments.

Growth conditions

Suspension cultures of *Nicotiana tabacum* Bright Yellow-2 cells were grown in liquid medium containing 4.6g/l M&S salts (Formedium), 30 g/l sucrose, 0.2 g/l KH_2PO_4, 1 mg/l Thiamine, 0.2 mg/l 2, 4-D and kept in the dark at 24°C with constant shaking. Cells were maintained by transferring 2 mL of one-week-old culture into a new flask containing 100 mL BY2 medium. Experiments were carried out using 2-3 day-old cells.

METHOD DETAILS

Generation of BY2 cells containing 35S::GFP-BASL and 35S::GFP

35S::GFP-BASL was generated using Golden Gate cloning [35], using the L2 backbone vector pICSL4723. Position 1 contained the pICSL11024 module, which confers Kanamycin resistance in plants, position 2 and 3 contained dummy modules (pICH54022 and

pICH54033) and position 4, the BASL-containing module (L1: EC71248), before an end linker (ELE-4-EC41780). The L1 BASL module was made up of the L0 'PU' 35S promoter (EC15058), GFP-BASL CDS as an 'SC' component (EC71137) and an Act-2 terminator (EC44300). Plasmid containing 35S::EGFP-nos was a kind gift from Christine Falkner [34].

Transient assays were carried out as described by [36]. Agrobacterium (strain GV3101) containing either *35S::GFP-BASL* or *35S::GFP* were mixed with 3-day-old BY-2 cells. The solutions were then spotted on to plates containing modified BY-2 media (4.6g/l M&S salt, 10 g/l sucrose, pH 5.8) with 0.4% phytagel. The plates were incubated for 2 days at 23°C in the dark. Experiments were carried out in duplicate.

For stable lines, agrobacterium containing *35S::GFP-BASL* was co-cultured with 3-day-old BY-2 cells for 2 days at 23°C in the dark. Co-cultures were washed with BY-2 liquid medium and spread onto plates containing BY-2 medium with 0.4% phytagel, 50 μg/mL kanamycin and 500 μg/mL carbenicilin. Resistant calli were transferred into BY2-medium containing 50 μg/mL kanamycin and 500 μg/mL carbenicilin. 5 independent calli were obtained and all contained cells expressing GFP-BASL in the same pattern.

Drug treatments

Stock solutions of 100 mM NPA, 100 mM TIBA (Sigma, T5910), 200 mM oryzalin (Sigma-Aldrich; 36182) and 10 mM latrunculin B (Abcam; 144291) were prepared in DMSO. The drugs were added to 1-day old cell cultures at final concentrations of 50 μM NPA, 5 μM TIBA, 10 μM oryzalin or 250 nM latruculin B. For experiments with NPA, BY-2 cultures were grown in the presence of 0.1 mg/L a-naphthalenacetic acid (NAA; Sigma-Aldrich; N1641,). The cell cultures were then imaged over several days. Experiments were repeated at least 3 times.

Labeling of cell walls

Cell walls were labeled by adding 0.005% (w/v) Direct Fast Red B (Sigma-Aldrich; R314188) to 2 mL of 3-day old suspension cell culture. The cells were collected by centrifugation (167.7 x g for 4 min) following a 30 min incubation and resuspended in protoplasting solution or culture medium.

Formation of protoplasts

Protoplasts were prepared from 3-day-old BY-2 cells. For making videos of cells becoming protoplasts, the cells were first stained with Direct Fast Red. The cells were resuspended in 12.5 mL of BY-2 protoplasting solution containing 2% of cellulase "Onozuka" R-10 (10 g, Yakult pharmaceutical Ind. Co. LTD, Tokyo, Japan), 0.05% of pectolyase Y-23 (Duchefa Biochemie; P8004.0001) and 0.4 M D-mannitol (Sigma-Aldrich, 63559). The protoplasts were collected by centrifugation after 3 h incubation on a shaker. Videos of cells forming protoplasts were made from an aliquot of the cells taken immediately after resuspension in protoplasting solution.

FM4-64 labeling of protoplasts

A 3.4 mM stock of FM4-64 (Invitrogen, T3166) was prepared in water. A working solution was made by adding 2 μL of the stock to 1 mL of BY2 medium containing 0.4 M mannitol. Washed protoplasts were mixed with an equal volume of the working solution. For rotation experiments, 500 μL of the protoplast-FM4-64 solution was mixed with 250 μL of warm 2% (w/v) low melting point agarose and then the solution placed in the center of a petridish.

Protoplast regeneration

Protoplast regeneration was carried out as described in [29]. Protoplasts were washed 3 times by centrifugation with FMS media [4.3 g/L MS-salts, 100 mg/L (myo)-inositol, 0.5 mg/L nicotinic acid, 0.5 mg/L pryoxidine-HCL, 0.1 mg/ L thiamine and 10 g/L sucrose, 0.25 M mannitol]. They were then transferred to FMS media supplemented with 0.1 mg/L NAA and 1.0 mg/L benzylaminopurine (Sigma-Aldrich; B3274). Protoplasts were then either imaged or placed in a cell culture plate incubated in the dark at 23°C.

Microscopy

Time-lapse imaging of cells and protoplasts was performed using a Bioimaging chamber [37, 38], with a Zeiss LSM 5 or Zeiss 880 exciter confocal laser scanning microscope equipped with a x20 air lens with a NA of 0.8. Z stacks were collected at a spacing of 2-4 μm. An interval of 10-60 min was used. Direct Fast Red was excited at 535 nm using an Argon ion laser and its emission collected at 595 nm. GFP was excited at 488 nm using an Argon ion laser and the emission collected at 495-530 nm.

All images were processed using ImageJ software (https://imagej.nih.gov/ij/) which contains tools for projecting z stacks, adjusting brightness and contrast, aligning movies, plot profile, extracting the cell's centroid, major and minor axes, and measuring angles. Montages were assembled using Adobe Photoshop.

QUANTIFICATION AND STATISTICAL ANALYSIS

The proportion of the nucleus inside the cell half containing polarized BASL was determined by measuring a displacement ratio. The value was determined by dividing the length of nucleus from the centroid toward the edge facing polarized BASL by the total length of the nucleus (See Figures S2A–S2C). (A value of 0.5 indicates no bias, > 0.5 indicates the nucleus is skewed toward the cell half containing GFP-BASL, and < 0.5 indicates the nucleus is skewed toward the end without GFP-BASL). Measurements were obtained from 2 replicates.

To determine the orientation of polarized BASL, protoplasts were divided into quadrants relative to the X-Y imaging plane (where quadrants 1-4 represented 12-3 o'clock, 3-6 o'clock, 6-9 o'clock and 9-12 o'clock, respectively). An orientation was assigned depending on the quadrant occupied by the cap center. Protoplasts with 2 caps of polarized BASL were given 2 scores. Protoplast with polarized BASL on their top surfaces were also scored. Images were obtained from 4 replicates.

The proportion of the protoplast occupied by polarized BASL was calculated using $2\pi rh/4\pi r^2$ = average 18% (stdev 1, min = 5, max = 42; n = 35); Using $\pi(a^2 + h^2)/4\pi r^2$ = average 17% (stdev 1, min = 4, max = 41; n = 35); Using $2\pi r^2(1\text{-}\cos\theta)/4\pi r^2$ = average 17% (stdev 1, min = 2, max = 39; n = 35), where h is the height of the cap, r is the radius, a is the radius at the base of the cap and θ is the polar angle. Protoplasts were analyzed from 3 independent experiments.

Chi square tests were performed at http://quantpsy.org/chisq/chisq.htm.

Current Biology, Volume *30*

Supplemental Information

Intrinsic Cell Polarity Coupled to Growth Axis Formation in Tobacco BY-2 Cells

Jordi Chan, Catherine Mansfield, Flavie Clouet, Delfi Dorussen, and Enrico Coen

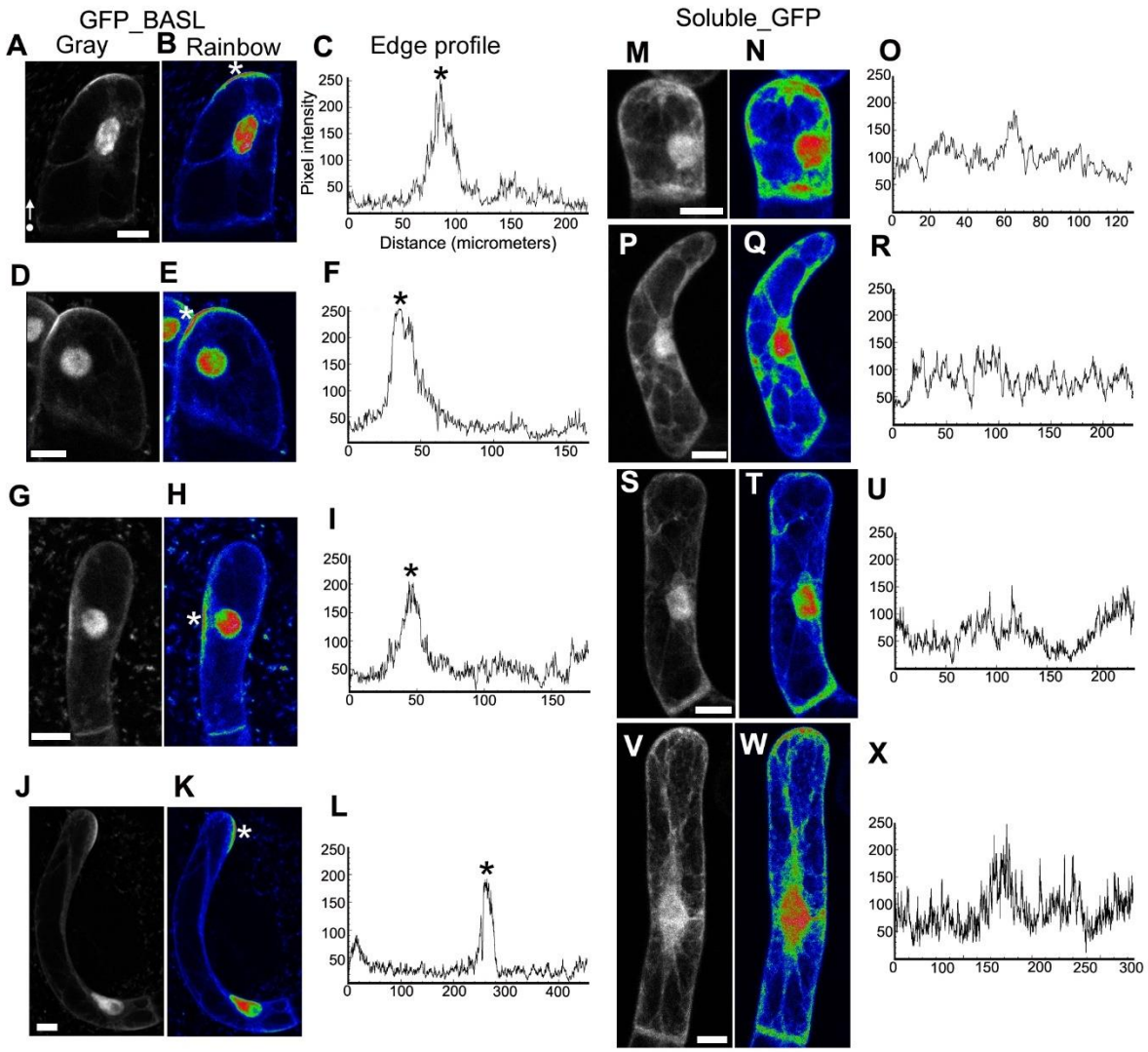

Figure S1: Localisation of 35S:GFP-BASL and 35S:GFP in BY-2 cells. Related to Figure 1.

(A,D,G,J) Examples of BY-2 cells transformed with GFP-BASL in transient assays. (B, E, H, K) Corresponding Rainbow LUT images. (C, F, I, L) Corresponding edge intensity/profiles. Note: GFP-BASL often labels the domed tips of terminal cells in filaments, though it may also label side walls (e.g. G, H, I). (M,P,S,V) Examples of BY-2 cells transformed with soluble GFP. (N,Q,T,W) Corresponding Rainbow LUT images. (O,R,U,X) Corresponding edge intensity profiles. Note in edge profiles, pixel intensities tend to be relatively high along cross-walls between cells (peaks on right-hand side of plots). The dot and arrow in (A) mark the origin and direction of the edge intensity profile, respectively. The asterisks mark polarised BASL. Bar = 15 µm.

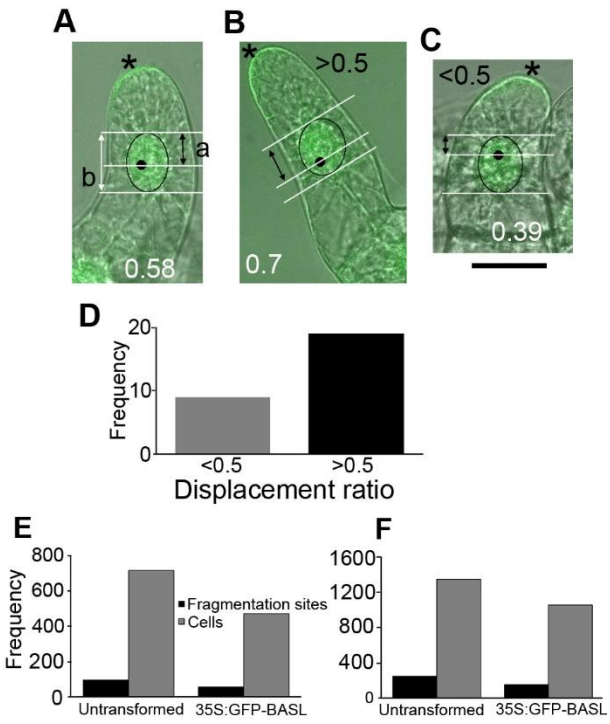

Figure S2: Properties of cells expressing 35S::GFP-BASL. Related to Figure 1.

(A-C) Images of premitotic cells expressing 35S::GFP-BASL taken 4 hours before mitosis showing their nuclei colocalise with cell's centroid (back spot). The nucleus overlapped the cell's centroid In 30/31 cells (obtained from 2 replicates) – although not centrally aligned with it in 28 cells. A displacement ratio was estimated for each of the 28 cells where the nucleus was not centrally aligned with the centroid. Cells were divided into two halves by drawing a line through the centroid (A). The proportion of the nucleus inside the cell half containing polarised BASL (asterisk) was estimated by dividing length a (distance between centroid line and edge line facing cell end with GFP-BASL; black arrows) by length b (total length of the nucleus; white arrows) (A). A value of 0.5 indicates the nucleus is centrally aligned, >0.5 indicates a greater proportion of the nucleus is inside the cell half with polarised BASL (B), and <0.5 indicating a greater proportion of the nucleus is inside the cell half without polarised BASL (C). Asterisks indicate cell end with polarised BASL. White numbers indicate the displacement ratio. Bar = 30 µm. (D) Histogram showing the displacement of the nuclei in the 28 cells, where the nucleus was not centrally aligned with the centroid. 19 cells had nuclei displaced towards, and 9 cells nuclei away from, the cell's end with polarised BASL. This distribution was not significantly different from a uniform distribution where there was an equal probability of being skewed towards either end of the cell (chi square = 3.571, p=0.06, 1 degree of freedom). (E-F) Plots showing the number of fragmentation sites in cells from untransformed or cultures expressing 35S:GFP-BASL (2 independent experiments). Cultures were quantified 4 days after subculture into fresh media. (Experiment 1 (E) = untransformed culture gave 95 fragmentation sites out of 718 cells, compared to 35S::GFP-BASL which gave 56 fragmentation sites out of 474 cells; Experiment 2 (F) untransformed culture gave 244 fragmentation sites out of 1347 cells, compared to 35S::GFP-BASL which gave 154 fragmentation sites out of 1052 cells). The frequencies of fragmentation sites in untransformed compared to transgenic cultures were not significantly different. [Experiment 1 (E): chi square = 0.40, p-value =0.53, 1 degree of freedom. Experiment 2 (F): chi square = 3.7, p-value =0.054, 1 degree of freedom].

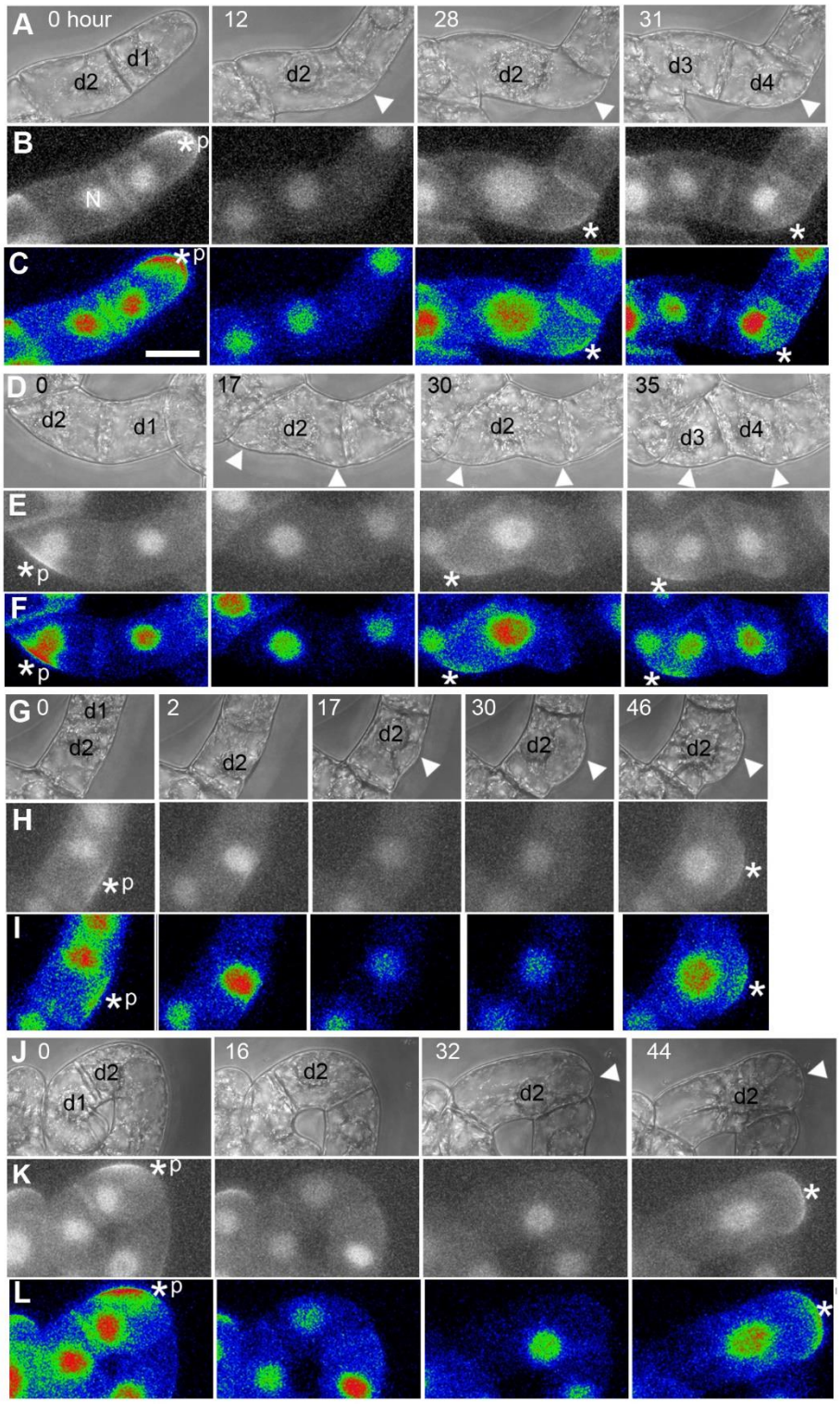

Figure S3: Examples of fragmentaion sites developing in filaments expressing 35S::GFP-BASL. Related to Figure 1.

Bright field (A, D, G, J) and corresponding GFP-BASL images (B, E, H, K) and Rainbow LUT images (C, F, I, L) showing temporal relationship between fragmentation and polarised BASL . Cells were tracked immediately after cell divison in daugher cells either without (A-C) or containing the parential BASL patch (D-L). (A -C) Polarised BASL patch is absent in internal daughter cell d2 (0 hours). A patch becomes prominent at the bulge in d2 (28 hours). Cell d2 then divides (31 hours) giving rise to cells

d3 and d4. (D-F) The parental BASL patch occupies a lateral site in daughter cell d2. The parental patch disappears (17 hours) and a new patch forms at the same site after a bulge forms (30 hours). The cell then divides (35 hours). Note: cell d2 forms another bulge on opposite side of the cell, which was not marked by parental BASL. (G-I) The parental patch of GFP-BASL occupies a lateral site in cell d2 (0 hours). It then disappears (2 hours) and a new patch forms after a bulge forms (46 hours). (J-L) The parental patch of GFP-BASL is located on a lateral face of cell d2 (0 hours). It disappears (16 hours) and a new patch appears at the new tip breaking from the filament axis (44 hours). Arrow head = fragmentation site, asterisk indicates polarised BASL, d1, d2 = daughter cells, d3, d4 = daughters of d2. Bar = 30 µm. t=0 refers to 56 (A-C), 59 (D-F), 93 (G-I), and 72 (J-L) hours after start of imaging.

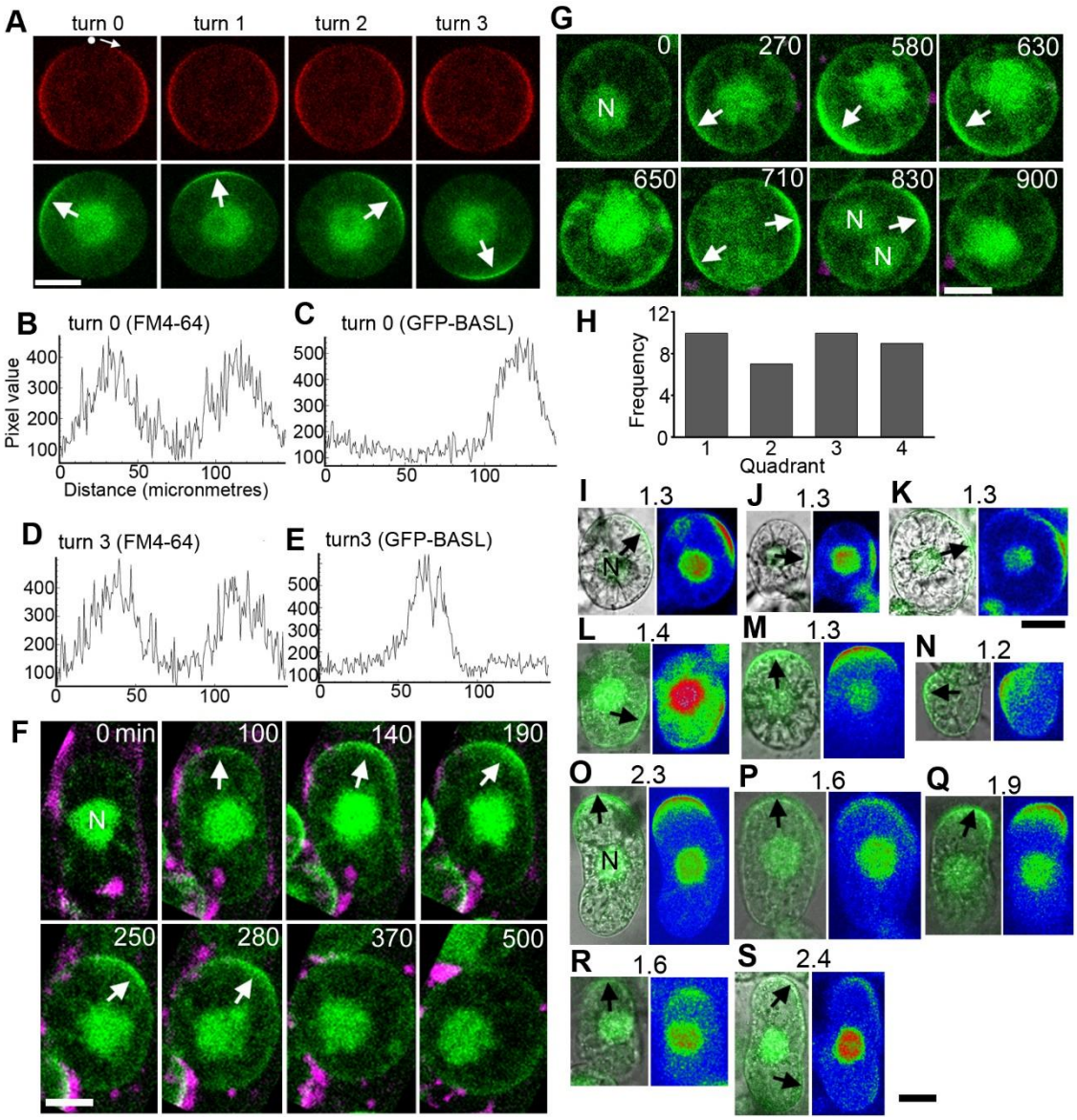

Figure S4. Behaviour of polarised BASL in protoplasts and regenerating protoplasts. Related to Figures 2 and 4.

(A) Rotation of protoplast stained with FM4-64 (red) and expressing GFP-BASL (green). The protoplast was turned 3 times (turn1-3), by rotating the sample. Note: the axial labelling pattern of FM4-64 is insensitive to turning, while GFP-BASL changes location. (B-E) Edge proile plots of the protoplast shown in A at turn 0 (B: FM4-64, C: GFP-BASL) and turn 3 (D: FM4-64, E: GFP-BASL). The axial labelling pattern of FM4-64 gives rise to 2 peaks (B,D). Polarised GFP-BASL displays a single peak (E,F). The location of the GFP-BASL peak changes location when the protoplast was turned; the FM4-64 peaks do not. (F) Appearance of GFP-BASL (green) during protoplast formation. GFP-BASL is initially present in the nucleus (0 min, N). A cap of polarised BASL then appears (100 min) and intensifies (140–280 min) before disappearing when the protoplast forms (500 min). The cell wall has been stained with Direct Fast Red B (magenta). (G) Polarised GFP-BASL shifting location in a dividing protoplast. GFP-BASL is initally present in the nucleus (0 h, N). A cap of polarised GFP-BASL

appears (270 min) at 8 o'clock. Polarised BASL disappears just before divison (650 min) and then reappears in a new postion (2 o'clock) after the nucleus has divided (830 min; note: 2 nuclei are present). The appearance of BASL at 2'oclock is preceded by a transitional state in which polarised GFP-BASL forms two caps at 8- and 2'oclock (710 min). Polarised GFP-BASL disappears after the daughter nuclei fuse into one structure (900 min). Note: cells in protoplasting solution do not form new cell walls following nuclear division. (H) Histogram showing the orientation of polarised BASL is not coordinated in protoplasts. 41 protoplasts were divided into quadrants within the imaging plane, 10 cap centres were in the first quadrant (12-3 o'clock; e.g. Figure 2D, protoplast a, 600 min), 7 in the second (3-6 o'clock, e.g. Figure 2D, protoplast c, 600 min), 10 in the third (6-9 o'clock; e.g. Figure 2D, protoplast d, 150 min) and 9 in the fourth (9-12 o'clock; e.g. Figure 2D, protoplast a, 150 min). This distribution is not significantly different from random (χ^2 for deviation from random orientation = 0.667, p=0.881, 3 degrees of freedom). Eight cells had a cap on the top surface (e.g. Figure 2D, protoplast c), which is consistent with a random distribution given that the cap occupies 18% of the protoplast surface area (7 out of 40 cells are expected to have a cap on the top surface if polarity is randomly oriented). Three of the 41 cells had two caps; two cells with both caps on their side surfaces and one with a cap on the top surface and the other on a side surface. (I-N) Polarised GFP-BASL displays diverse orientations in ovoid-shaped cells with relatively low aspect ratios. Left-hand panels show merge of bright field and GFP-BASL channels. The right-hand panels show corresponding Rainbow LUT images (of the GFP channel). Numbers indicate aspect ratio. Out of 40 cells with relatively low aspect ratios (1.1 to 1.5), 20 and 18 cells had polarised BASL on long or short sides, respectively. The numbers for short versus long side was not significantly different (χ^2 for deviation from random orientation = 0.4, p=0.527, 1 degree freedom). (O-R) Polarised GFP-BASL tends to be on one of the short sides of sausage-shaped cells with relatively high aspect ratios. 19/20 cells with higher aspect ratios (1.6 to 3.2) had polarised BASL only on a short side. The bias for short versus long side was significant (χ^2 for deviation from random orientation =16.2, p=0.00006, 1 degree freedom). Measurements were obtained from 3 replicates. (S) Example of polarised BASL located on both a long and short side of sausage-shaped cell. Arrows mark polarised GFP-BASL. Bar: A, I-N = 20 µm; F-G = 15 µm; O-S = 30 µm. t=0 in panels F,G is a few minutes after resuspension in protoplasting solution. See also Video S2.